

Remote geological mapping using 3D photogrammetry: an example from Karrat, West Greenland

Erik Vest Sørensen and Pierpaolo Guarnieri

The geology of the Palaeoproterozoic Karrat Group in West Greenland (71°–74°50' N) was investigated during the field seasons 2015–2017, using a combination of digital photogrammetry and traditional field work in a collaboration between the Geological Survey of Denmark and Greenland and the Ministry of Minerals Resources of Greenland. The area is characterised by steep alpine terrain with more than 2000 m of relief that in many places is completely inaccessible, which makes field work extremely difficult. Therefore 3D mapping using digital photogrammetry is an invaluable tool in the investigation of the region. Early geological investigations of the area involved the first use of photogrammetry in Greenland (Henderson & Pulvertaft 1987). This contribution serves as an example of the present-day use of photogrammetry in geological interpretation, following the workflow outlined in Sørensen & Dueholm (2018). During the last three years, more than 50 000 stereo images have been collected using handheld, calibrated digital cameras while conducting field work in the area (Rosa *et al.* 2016, 2017, 2018). The images, which cover large parts of the steep cliff sections in which the geology is superbly exposed, are essential to the ongoing revision of the geological map sheets covering the area. Here we present a small subset of the data from the island of Karrat (Fig. 1), showcasing the potential

of 3D geological mapping in Greenland as well as presenting new insights into the geology of the Karrat Group.

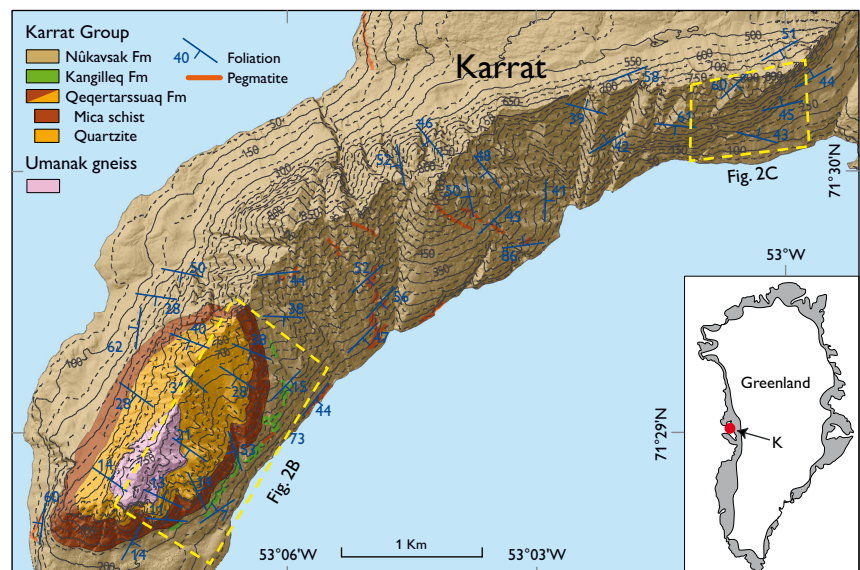
Regional Geology

The Karrat region is part of the Rinkian fold belt of West Greenland (Henderson & Pulvertaft 1967). The area mainly consists of reworked Archaean gneisses overlain by supracrustal successions of the Palaeoproterozoic Karrat Group. The group initially comprised two formations: the Qeqertarsuaq and Nûkavsak Formations, but was later extended to also include the Marmorilik Formation (Henderson & Pulvertaft 1987), originally considered to be of Archaean age but later shown to be Palaeoproterozoic and resting with a depositional unconformity on Archaean gneiss (Garde 1978). The Karrat Group and its Archaean basement were metamorphosed and folded during the Rinkian orogeny *c.* 1.9–1.8 Ga (Henderson & Pulvertaft 1987; Grocott & Pulvertaft 1990).

Data acquisition and preparation

Stereo images were collected with calibrated, hand-held digital SLR cameras from a boat (which served as base-camp) and from a helicopter used for day excursions and to sup-

Fig. 1. Part of the new geological map of Karrat island (location in Greenland marked on inset map), prepared as part of an ongoing revision of the 1:100 000 scale regional geological map sheets. The digital elevation model was generated from the oblique stereo-images collected during field work. Inset boxes show the approximate positions of Figs 2B, C.



port field camps. The images were typically collected while moving along the cliff faces in straight or gently curving trajectories tens to hundreds of kilometres long at varying distances to the cliffs. We here present results from a subset of the images collected from boat and helicopter flights around Karrat. We used a hand-held Nikon D800E (36 megapixel) digital, single lens reflex camera equipped with a Carl Zeiss Distagon 35 mm lens that was pointed perpendicularly to the slope of interest through an open helicopter window or from boat. With the images we have almost complete coverage of the island with a resolution of c. 0.1–0.5 m (pixel size on the ground).

The images were prepared for 3D mapping following the exact workflow of Sørensen & Dueholm (2018). GPS positional data collected together with the images during field work were used as a first approximation for absolute positioning. The absolute orientation was subsequently refined through a proper bundle adjustment also including pass points measured stereoscopically in monochrome aerial photographs on a scale of 1:150 000 (i.e. points also identified in the oblique stereo-images), as well as planar levelling points (sea-level points) measured in the oblique images. The absolute accuracy of the stereoscopic models is around 3 m (xyz) while the photogrammetric or relative accuracy is in the millimetre to centimetre range.

The images were subsequently used to extract elevation data for Karrat, using SURE software from Nframes. A digital elevation model of Karrat island with a 2 × 2 m grid (Fig. 1) was produced to assist in the geological interpretation, as well as a so-called point cloud (a set of data points in 3D space representing the terrain surface) of the island to be used for visualisation purposes (Fig. 2A).

Data interpretation – 3D mapping

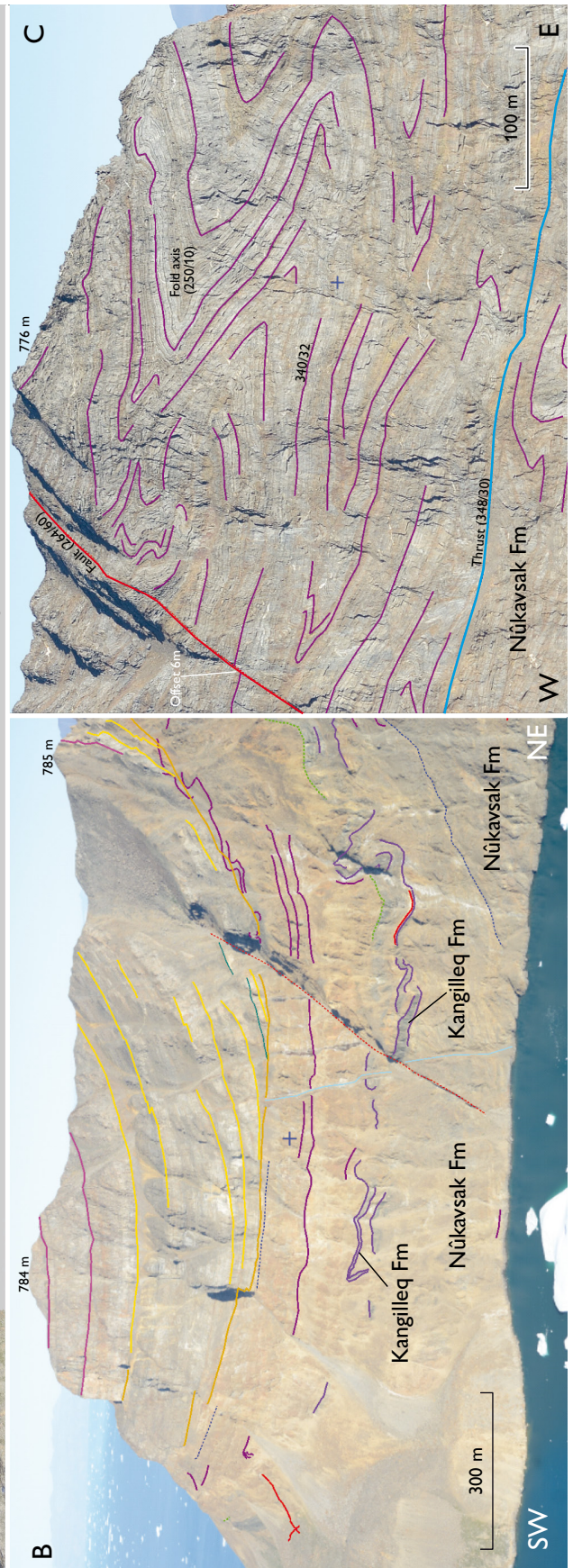
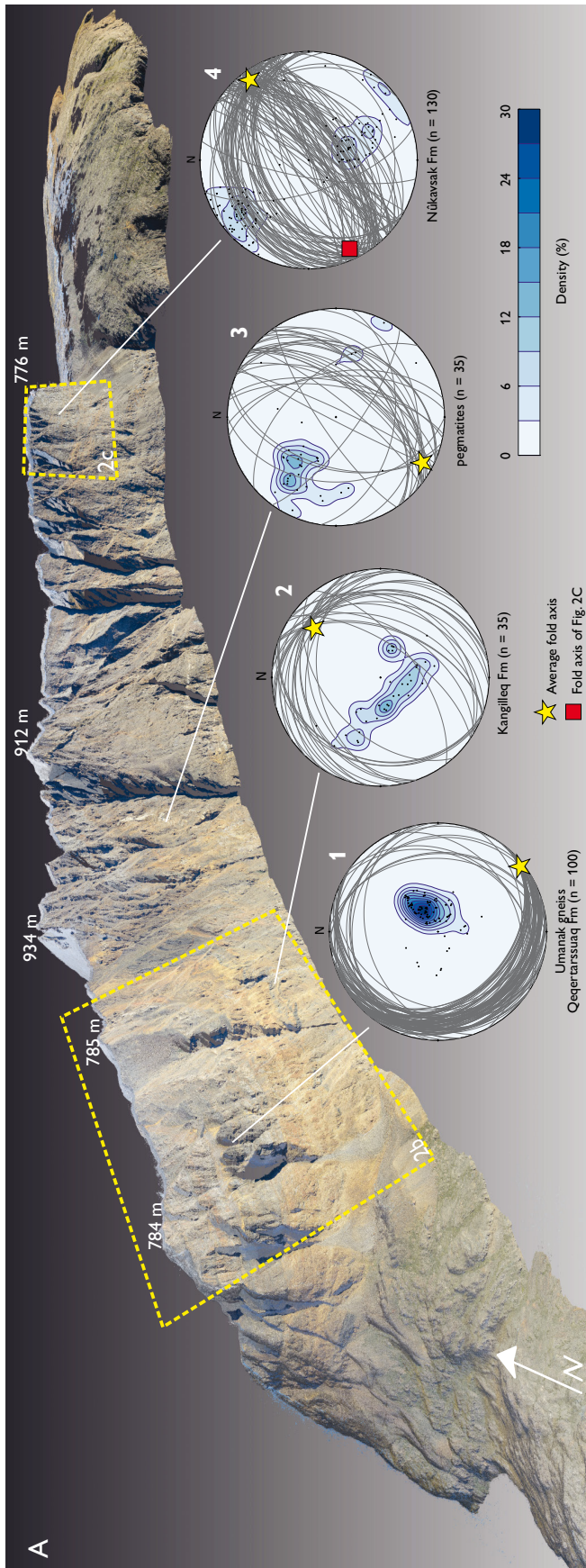
With the images properly oriented in 3D, essentially all corners of the island can be visited stereoscopically with the ease of a mouse-click and a geological interpretation can be performed. In this way it is possible, so to speak, to bring the rock exposures into the laboratory where the geology can be analysed. Whereas previous geological investigations have taken place in the more accessible lower parts of Karrat, here we focus on the inaccessible, higher parts of the island. Karrat represents the north-westernmost exposure of the Kigarsima Nappe (Henderson and Pulvertaft 1987). The south-western top of the island displays the overturned basement core of this tectonic nappe that forms an inverted sequence of Archaean banded gneiss (Umanak gneiss) with amphibolite layers sitting structurally on top of garnet-mica schist and quartzite of the Qeqertarsuaq Formation, metavolcanic

rocks of the Kangilleq Formation and biotite schist of the Nûkavsak Formation (Fig. 2).

In addition to the actual 3D mapping with tracing of geological units, bedding and foliation (Figs 2B, C), a powerful feature of the 3D mapping tool is the possibility to gather structural data remotely. This makes it possible to extend structural information from the shoreline, from where most structural data are usually collected during field work, up to outcrops at the top of the mountain (Fig. 2A). This is important as it gives a more complete data coverage, and because the Karrat region is structurally complex with multiple deformation stages (Henderson & Pulvertaft 1987; Grocott & McCaffrey 2017).

The structural data obtained with 3D photogrammetry consist of strike and dip of bedding/foliation, faults and thrusts together with traces of the geological boundaries between lithological or lithostratigraphic units. The data are stored as points (vertexes) along vectorised lines, so-called polylines. The strike and dip measurements presented here were calculated for each vertex of the polylines obtained through the 3D mapping as a moving average of best fitted planes by least square adjustment. More specifically, for each individual vertex a search window including seven adjacent vertexes was used in the calculation. In this way strike and dip measurements were generated for all vertexes of the mapped polylines. The measurements were subsequently filtered based on the standard deviation of each measurement. The result of this is a dataset of georeferenced points with calculated strikes and dips of their associated planar surfaces, which can be plotted on a geological map and analysed using stereoplots (Fig. 2). The Karrat island dataset consists of foliation in the Umanak gneiss and amphibolites, bedding/foliation in quartzites of the Qeqertarsuaq Formation, bedding of folded metavolcanic rocks of the Kangilleq Formation and the intensely folded metagreywacke strata of the Nûkavsak Formation, as well as folded pegmatites.

Fig. 2. Point cloud model of Karrat, looking north. **A:** Lower hemisphere stereographic plots 1–4 of foliation and bedding measurements obtained from 3D polylines and shown as pole-to-bedding great circles and density averages. Average fold axis orientations are defined by the intersection of great circles, shown with stars on the individual stereoplots. **B:** Structural data from the southern part of the Karrat showing the overturned limb of the Kigarsima Nappe (Umanak gneiss and Qeqertarsuaq Formation), folded metavolcanic rocks of the Kangilleq Formation and Nûkavsak Formation metagreywackes. **C:** Detailed close-up of the intense kink folds (purple lines) in the Nûkavsak Formation (numbers indicate dip direction/dip angle. Blue line at the base: thrust fault dipping 30°NW compatible with the average fold trends. Red line: normal fault dipping 60°W with a measured offset of 6 m.



Previously, Grocott and McCaffrey (2017) described the emplacement of the Kigarsima Nappe towards ENE as established by structural analysis of stretching lineations along a basal thrust contact. The authors also described an intersection lineation between cleavage and bedding, gently plunging towards SW, which appears to be compatible with a stretching lineation defined by hornblende and biotite minerals oriented WNW–ESE that they related with a later top-to-NW tectonic transport overprinting the Kigarsima structures.

Our new data presented in Fig. 2 are in good agreement with the observations of Grocott and McCaffrey (2017). At Karrat island only the lower limb of the Kigarsima Nappe is preserved, represented by the Umanak gneiss and Qeqertarsuaq Formation (Fig. 2B). The *c.* 100 new foliation measurements (Fig. 2 stereoplot 4) calculated from the mapped 3D polylines (Fig. 2B) describe the geometry of a large recumbent fold with a subhorizontal, NNW–SSE- to NW–SE-trending fold axis. This structural trend is compatible with ENE–WSW to NE–SW compression that is consistent with the ENE- to NE-tectonic transport suggested by Grocott and McCaffrey (2017). In contrast, a different structural trend is observed in the younger lithostratigraphic units. From the structural data (Fig. 2A stereoplots 1–3) it appears that the structural trends are rotated almost 90°. In fact, the 40 measurements obtained from the folded metavolcanic rocks of the Kangilleq Formation (Fig. 2A stereoplot 2) located in the overturned limb of the Kigarsima Nappe show an average NE-plunging fold axes that is similar to the fold axes obtained from the 130 measurements (Fig. 2A stereoplot 4) from the large kink folds observed in the Nûkvsak Formation (Fig. 2C). These trends of folds are compatible with NW–SE compression that in turn seems to be consistent with the top-to-NW tectonic transport indicated by Grocott and McCaffrey (2017). Similar fold axis trends are observed in the mapped pegmatites that cut the stratigraphy in the central part of the island (Figs 1 and 2A stereoplot 3). This establishes an important cross-cutting relationship between the folding event and the pegmatites which are probably related to high temperature metamorphism dated at *c.* 1830 Ma (Rosa *et al.* 2017; Kirkland *et al.* 2017).

Summary

This study demonstrates how 3D mapping can be used for geological mapping in remote and inaccessible areas such as Greenland following the procedures of Sørensen & Dueholm (2018). This is done with an example from the island of Karrat, West Greenland. Using just a digital camera, we have

generated a new revised geological map of Karrat including topography, geology and structural data. Our approach and methodology offer great support to standard field work where detailed outcrop information can be extended into regional-scale mapping.

Acknowledgments

This work was carried out within the framework of an ongoing project financed by the Geological Survey of Denmark and Greenland and the Ministry of Mineral Resources of Greenland. We thank Asger Ken Pedersen and Ken McCaffrey for the helpful comments and suggestions.

References

- Garde, A.A. 1978: The Lower Proterozoic Marmorilik Formation, east of Marmorilik, West Greenland. *Meddelelser om Grønland* **200**(3), 71 pp.
- Grocott, J. & Pulvertaft, T.C.R. 1990: The Early Proterozoic Rinkian belt of central West Greenland. In: Lewry, J.F. & Stauffer, M.R. (eds): The Early Proterozoic Trans-Hudson Orogen of North America. Geological Association of Canada, Special Paper **37**, 443–463.
- Grocott, J. & McCaffrey, K.J.W. 2017: Basin evolution and destruction in an Early Proterozoic continental margin: the Rinkian fold–thrust belt of central West Greenland. *Journal of the Geological Society (London)* **174**, 453–467.
- Henderson, G. & Pulvertaft, T.C.R. 1967: The stratigraphy and structures of the Precambrian rocks of the Umanak area, West Greenland. *Meddelelser Dansk Geologisk Forening* **17**, 1–20.
- Henderson, G. & Pulvertaft, T.C.R. 1987: Geological Map of Greenland, 1:100 000, Marmorilik 71 V.2 Syd, Nûgâtsiaq 71 V.2 Nord, Pangnertôq 72 V.2 Syd. Descriptive text. 72 pp., 8 plates. Copenhagen: Geological Survey of Greenland.
- Kirkland, C.L., Hollis, J., Danišik, M., Petersen, J., Evans, N. J., & McDonald, B.J. 2017: Apatite and titanite from the Karrat Group, Greenland; implications for charting the thermal evolution of crust from the U–Pb geochronology of common Pb bearing phases. *Precambrian Research* **300**, 107–120.
- Rosa, D., Guarnieri, P., Hollis, J., Kolb, J., Partin, C., Petersen, J., Sørensen, E.V., Thomassen, B., Thomsen L. & Thrane, K. 2016: Architecture and mineral potential of the Paleoproterozoic Karrat Group, West Greenland. *Danmarks og Grønlands Geologiske Undersøgelse Rapport* **2016/12**, 98 pp.
- Rosa, D., Dewolfe, M., Guarnieri, P., Kolb, J., LaFlamme, C., Partin, C., Salehi, S., Sørensen, E.V., Thaarup, S., Thrane, K. & Zimmermann, R. 2017: Architecture and mineral potential of the Paleoproterozoic Karrat Group, West Greenland – Results of the 2016 Season. *Danmarks og Grønlands Geologiske Undersøgelse Rapport* **2017/5**, 98 pp.
- Rosa, D., Bernstein, S., Dewolfe, M., Dziggel, A., Grocott, J., Guarnieri, P., Kolb, J., Partin, C., Sørensen, E.V. & Zimmermann, R. 2018: Architecture and mineral potential of the Paleoproterozoic Karrat Group, West Greenland – Results of the 2017 Season. *Danmarks og Grønlands Geologiske Undersøgelse Rapport* **2018/23**, 102 pp.
- Sørensen, E.V. & Dueholm, M.: 2018: Analytical procedures for 3D mapping at the Photogeological Laboratory of the Geological Survey of Denmark and Greenland. *Geological Survey of Denmark and Greenland Bulletin* **41**, 99–104 (this volume).

Authors' address

Geological Survey of Denmark and Greenland, Øster Voldgade 10, DK-1350 Copenhagen K, Denmark. E-mail: evs@geus.dk.